



## Solid-State Study of Rifaximin in Organic Solvents

M. Ángeles Peña<sup>1</sup>, M. Buhagiar<sup>2</sup>, N. Borg<sup>2</sup>

<sup>1</sup>Unidad Docente de Farmacia y Tecnología Farmacéutica, Facultad de Farmacia, Universidad de Alcalá, Alcalá de Henares, E-28871 Madrid, Spain

<sup>2</sup>Department of Pharmacy, Faculty of Medicine and Surgery, Biomedical Sciences Building, University of Malta, Msida, MSD2080, Malta

**Corresponding author: M. Ángeles Peña**, Facultad de Farmacia, Universidad de Alcalá, Alcalá de Henares, E-28871 Madrid, Spain. Tel: 918854611; Fax 918854658; E-mail: [angeles.pena@uah.es](mailto:angeles.pena@uah.es).

**Received:** March 08, 2023; **Accepted:** May 05, 2023; **Published:** May 12, 2023

© **Copyright 2023:** Pena et al. This is an open access article distributed under the terms of the Creative Commons Attribution License [CC-BY 4.0.], which permits unrestricted use, distribution, and reproduction in any medium, provided the original author and source are credited.

### Abstract

The objective of this paper was to study the behavior of rifaximin crystals obtained by solvent evaporation crystallization processes. The solid phases obtained were characterized and studied by thermal analysis and infrared spectroscopy. These studies are very important to know and analyses the polymorphic forms of drugs. From the results, all possible polymorphic forms can be identified and the most suitable one chosen according to its dissolution rate and bioavailability.

**Keywords:** Rifaximin; Thermal analysis; Polymorphism; physicochemical properties

### Introduction

Rifaximin (CAS 80621-81-4, molecular formula  $C_{43}H_{51}N_3O_{11}$  and molar mass  $785.891 \text{ g}\cdot\text{mol}^{-1}$ ), Figure 1 is a broad-spectrum antibiotic licensed for gastrointestinal and hepatobiliary diseases involving both gram-negative and gram-positive anaerobic and aerobic enteropathogens, such as noninvasive strains of *Escherichia coli* in Traveller's diarrhoea across all ages, treatment of irritable bowel syndrome with diarrhoea (IBS-D) in adults and prophylactic treatment of over hepatic encephalopathy recurrence in adults [1-3]. It has poor systemic absorption, contributing to a negligible bioavailability of 0.4% that is structurally related to the addition of the benzimidazole ring to rifampin, a rifamycin derivative [4]. These pharmacokinetics limit rifaximin mode of action to only treating local gastroenterological tract pathogens hence providing a favourable side effect profile, and advantageous minimal microbial resistance [1,5].

Rifaximin has been widely associated with possession of minimal bioavailability; however, a breakthrough discovery revealed that bioavailability of rifaximin is dependent on the polymorphic form, hence certain forms exhibit more bioavailability compared to the other forms [9]. Polymorphism refers to the ability of a molecule to change conformation into various crystalline structures, depending on changes in temperature and/or pressure that causes spontaneous arrangement of molecules into regular/irregular geometric solids [9-11].

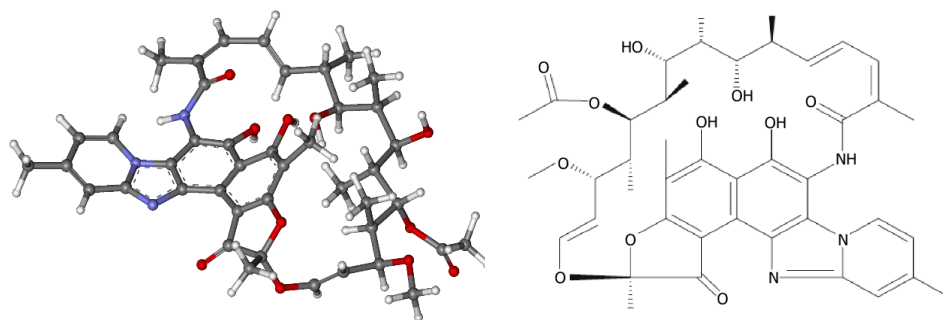


**Figure 1:** Chemical structure of rifaximin [6]. 3D ball-and-stick model of rifaximin molecule.

At least eight crystal phases have been described for rifaximin, named  $\alpha$ ,  $\beta$ ,  $\gamma$ ,  $\delta$ ,  $\epsilon$ ,  $\zeta$ ,  $\eta$ , and  $\iota$  being  $\alpha$  and  $\beta$  most represented forms, and apart from the polymorphs, the amorphous form of rifaximin possess different physicochemical properties, with the latter being systematically more bioavailable compared to the  $\alpha$ -form [12-16]. The most thermodynamically stable form, polymorph  $\alpha$ , is the one used commercially [17]. These polymorphic forms show among their properties a great difference in terms of intrinsic dissolution and adsorption in vivo. The solid forms can be chosen to select the best characteristic physical properties, e.g. dissolution rate and bioavailability. Rifaximin  $\alpha$  is the polymorphic form with the lowest systemic bioavailability and is the one on the market.

Different polymorphs can possess different physicochemical properties regarding stability, solubility and dissolution rates. These contrasting properties give rise to the requirement of proper distinguishing between the rifaximin polymorphs for improvement of already marketed polymorph and potential introduction of new polymorph, possessing contrasting properties to the previously marketed polymorph. As previously mentioned, differences in the pharmacokinetics of the crystalline forms of rifaximin alter pharmacological efficacy and safety, especially within patients with chronic diseases of immunodeficiency and leaky gut, that would require long-term rifaximin therapy. Various methods are currently used to obtain polymorphic drug forms, including multi-solvent sublimation, crystallization, lyophilisation, spray drying, or grinding [18,19].

Since it is known that the morphology of drug polymorphs play a key role for their application in the preparation of a drug, it is crucial to elucidate their structure, for this, different techniques crystallography, spectroscopy, microscopy and thermal techniques are available, such as crystal X-ray diffraction, nuclear magnetic resonance (NMR), Raman spectroscopy, Fourier-transform infrared spectroscopy (FT-IR), differential scanning calorimetry (DSC) or thermogravimetric analysis (TGA).

In this work, DSC, TGA and FT-IR have been used to determine physicochemical properties about the kinetic parameters of

rifaximin crystals, obtained using the crystallization process by evaporation of the each pure solvents [20].

## Material and Methods

### Materials

Rifaximin (mass fraction purity > 0.999) was supplied from Laboratories Liconsa (Guadalajara, Spain). Distilled water, cyclohexane, ethyl acetate, ethylene glycol, ethanol, acetone and 1,4-Dioxane, were acquired from assorted chemical suppliers. The detailed specifications regarding the materials are listed in Table 1.

**Table 1:** Properties of solvents used in the completed study.

Chemical name	Molecular formula	Molar mass ( $\text{g}\cdot\text{mol}^{-1}$ )	Source	Purity v/v (%)
Acetone	$\text{C}_3\text{H}_6\text{O}$	58.08	Panreac Química S.L.U (Barcelona, Spain)	99.5
1,4-Dioxane	$\text{C}_4\text{H}_8\text{O}_2$	88,11	Panreac Química S.L.U (Barcelona, Spain)	99.5
Ethyl acetate	$\text{C}_4\text{H}_8\text{O}_2$	88.11	Merck KGaA (Darmstadt, Germany)	99.5
Ethanol	$\text{C}_2\text{H}_5\text{OH}$	46.07	Scharlab (Barcelona, Spain)	>99.9
Water	$\text{H}_2\text{O}$	18.02		
Ethylene glycol	$\text{C}_2\text{H}_6\text{O}_2$	62.07	Panreac Química S.L.U (Barcelona, Spain)	99.5
Cyclohexane	$\text{C}_6\text{H}_{12}$	84.16	Scharlab (Barcelona, Spain)	99.5

### Solid phase preparation

Excess rifaximin was suspended in selected pure solvents to obtain a supersaturated solution. Sealed dark glass flasks containing a small excess of powder in the pure solvents were shaken in a temperature-controlled bath (HETO® Type SBD50-1 bio. 501828H, France) at  $T = 298.15 \text{ K} (\pm 0.1 \text{ K})$  and  $p = 0.1 \text{ MPa}$ , through 4 days and advanced calculating the saturation time. Suspensions were filtered (Durapore membranes  $0.2 \mu\text{m}$  pore size, Germany), and the solvent excess was gently evaporated at room temperature to prevent the removal of solvent loosely bound to the crystals that may affect the thermal behaviour of the solid phase and to ensure complete solvent evaporation. When the residues were dry, the crystals were collected in separate containers.

### Differential Scanning Calorimetry (DSC)

Differential scanning calorimetry analysis was performed with the Mettler TA 4000 DSC Star System equipment combined with the StarE software (Switzerland). For the analysis, aluminium crucibles of 40–100  $\mu\text{L}$  capacity were used. Samples weighing approximately 5 mg were examined using several heating rates;  $5^\circ\text{C}/\text{min}$ ,  $10^\circ\text{C}/\text{min}$  and  $20^\circ\text{C}/\text{min}$  under dynamic nitrogen gas purge (20 mL/min) by means of closed and pierced sample pans. Thermograms were obtained from  $25^\circ\text{C}$  to  $250^\circ\text{C}$  to obtain the complete thermogram and observe the behaviour of the drug in a large temperature range, including possible endothermic or exothermic effects above fusion. The melting or decomposition onset temperature is used throughout the analysis, so that mass

does not influence the result. Each measurement was performed in triplicate to calculate the heat of fusion  $\Delta H^f$  ( $Jg^{-1}$ ), which is the quantity of heat necessary to change 1 g of a sample in a solid state to the liquid state with no temperature change. Likewise, DSC testing was carried out, using the following standardized cycle with diverse temperature ranges, conditions of heating and cooling, and heating and cooling rates Table 2. All cycles were carried out using dynamic conditions unless otherwise specified.

**Table 2:** Conditions standardised cycle.

Test number	Cycles conducted per test, expressed in temperature ( $^{\circ}C$ ) and heating rate ( $^{\circ}C/min$ )
A	<ol style="list-style-type: none"> <li>1. 25 to <math>196^{\circ}C</math> at rate of <math>10^{\circ}C/min</math></li> <li>2. <math>196</math> to <math>25^{\circ}C</math> at rate of <math>-40^{\circ}C/min</math></li> <li>3. 25 to <math>196^{\circ}C</math> at rate of <math>10^{\circ}C/min</math></li> </ol>
B	<ol style="list-style-type: none"> <li>1. 25 to <math>196^{\circ}C</math> at rate of <math>10^{\circ}C/min</math></li> <li>2. <math>196</math> to <math>25^{\circ}C</math> at rate of <math>-5^{\circ}C/min</math></li> <li>3. 25 to <math>196^{\circ}C</math> at rate of <math>10^{\circ}C/min</math></li> </ol>
C	<ol style="list-style-type: none"> <li>1. 25 to <math>196^{\circ}C</math> at rate of <math>10^{\circ}C/min</math></li> <li>2. <math>196</math> to <math>25^{\circ}C</math> at rate of <math>-5^{\circ}C/min</math></li> <li>3. 25 to <math>260^{\circ}C</math> at rate of <math>10^{\circ}C/min</math></li> </ol>
D	<ol style="list-style-type: none"> <li>1. 25 to <math>196^{\circ}C</math> at rate of <math>10^{\circ}C/min</math></li> <li>2. <math>196</math> to <math>-10^{\circ}C</math> at rate of <math>-50^{\circ}C/min</math></li> <li>3. <math>-10</math> to <math>260^{\circ}C</math> at rate of <math>10^{\circ}C/min</math></li> </ol>
E	<ol style="list-style-type: none"> <li>1. 25 to <math>200^{\circ}C</math> at rate of <math>10^{\circ}C/min</math></li> <li>2. <math>200</math> to <math>-10^{\circ}C</math> at rate of <math>-60^{\circ}C/min</math></li> <li>3. <math>-10</math> to <math>260^{\circ}C</math> at rate of <math>10^{\circ}C/min</math></li> </ol>
F	<ol style="list-style-type: none"> <li>1. 25 to <math>200^{\circ}C</math> at rate of <math>10^{\circ}C/min</math></li> <li>2. <math>200^{\circ}C</math> for 15 minutes using isodynamic conditions</li> <li>3. <math>200</math> to <math>-10^{\circ}C</math> at rate of <math>-60^{\circ}C/min</math></li> <li>4. <math>-10</math> to <math>260^{\circ}C</math> at rate of <math>10^{\circ}C/min</math></li> </ol>
G	<ol style="list-style-type: none"> <li>1. 25 to <math>200^{\circ}C</math> at rate of <math>10^{\circ}C/min</math></li> <li>2. <math>200</math> to <math>-10^{\circ}C</math> at rate of <math>-80^{\circ}C/min</math></li> <li>3. <math>-10</math> to <math>260^{\circ}C</math> at rate of <math>10^{\circ}C/min</math></li> </ol>
H	<ol style="list-style-type: none"> <li>1. 25 to <math>200^{\circ}C</math> at rate of <math>5^{\circ}C/min</math></li> <li>2. <math>200</math> to <math>-10^{\circ}C</math> at rate of <math>-80^{\circ}C/min</math></li> <li>3. <math>-10</math> to <math>260^{\circ}C</math> at rate of <math>10^{\circ}C/min</math></li> </ol>

### Thermogravimetric analysis (TGA)

The thermal stability of rifaximin was investigated by thermogravimetric analysis (TGA) using TGA55 (EQU) equipment. The

experiments were carried out in aluminium crucibles (80  $\mu\text{L}$ ) at a heating rate of  $10^\circ\text{C}/\text{min}$  under nitrogen atmosphere. TGA/DTG curve was obtained in the temperature range of  $25\text{--}250^\circ\text{C}$  on a sample of approximately 10 mg.

#### Fourier transforms infrared spectroscopy (FT-IR)

The Fourier transform infrared spectroscopy (FT-IR) analysis was performed with the equipment Fourier Spectrum 2000 spectrometer Perkin Elmer System 20000FT-IR (EEUU) with a resolution of  $1\text{ cm}^{-1}$ . For the analysis, a 2:98 dilution with KBr (sample to analyse: KBr) is homogeneously mixed in agate mortar. This mixture is placed in a hydrostatic press and means of high pressure (10 T for 3 min), producing 10 mm diameter.

### Results and Discussion

DSC, TGA and FT-IR techniques offer interesting opportunities for the characterization of polymorphic forms of rifaximin. Karl Fischer titration was used water determination; a value of 1.3 % w/w was obtained.

#### Thermal stability analysis

The thermal properties of pure rifaximin original powder and of each solid phases in seven pure solvents were characterised using a DSC and TGA analysis.

**Table 3:** DSC for original powder.

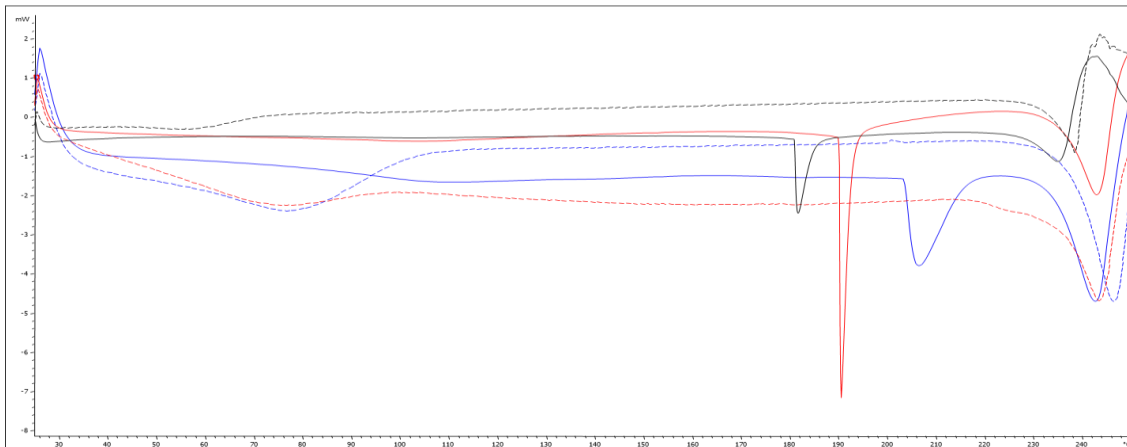
	Sealed	Non-sealed	Sealed	Non-sealed	Sealed	Non-sealed
Heating rate ( $^\circ\text{Cmin}^{-1}$ )	5		10		20	
Mass (mg)	4.4	3.7	4.9	3.9	4.7	4.1
Onset ( $^\circ\text{C}$ )	185.87	221.36	198.92	223.14	203.34	226.86
Peak ( $^\circ\text{C}$ )	186.62	-	199.46	-	206.46	-
$\Delta H^f$ ( $\text{Jg}^{-1}$ )	11.49	-	12.25	-	9.65	-

Table 3 and Figure 2 describes the results and thermo-grams obtained using different conditions, specially selecting various heating rates, which undoubtedly contribute to the detection of the formation of possible polymorphic forms. After carrying out different DSC, it was verified that the most satisfactory conditions were at  $10^\circ\text{C}/\text{min}$  and using hermetically closed pans. The greater the heating rate, the greater the area of the melting peak obtained. Then, the perforated samples obtained different DSC compared to the closed samples, they are observed a higher temperature at the beginning of the melting, due to the evaporation of the water and that could have led to the inter-conversion of rifaximin from one polymorph to another, which would explain the increase in the melting initiation temperature.

The DSC spectrum of rifaximin showed a peak of fusion (onset) at  $199^\circ\text{C}$ , compared to literature where the melting point of licensed rifaximin lies between  $216$  and  $221^\circ\text{C}$  or on around  $209^\circ\text{C}$  [21-23]. As observed in the results the thermal behaviours of pure drug rifaximine is very diverse and changing depending on the experimental conditions of the calorimetric study.

The thermogravimetry curve (TGA) as well as the derivative thermogravimetry (DTG) of the pure drug is shown in Figure 3 in the TGA curve, no water loss was observed, probably due to its high hydrophobicity. Any stage of weight loss evident in the curve was detected and at approximately  $240.0^\circ\text{C}$ , it can detect the water loss of rifaximin, with a weight variation of 6.6% due

to the decomposition of the drug, which is possibly due to presence of water and other solvents in the drug structure. DTG curve shows broad peaks in the range of 230 to 250 °C that were not separable. This phenomenon was consistent with the data from the DSC analysis, confirming the absence of pseudopolymorphism.



**Figure 2:** DSC spectrum of rifaximin using heating rates 5°C/min (black), 10°C/min (red) and 20°C/min (blue), using pierced sample pans (dotted lines) and closed sample pans (solid lines).

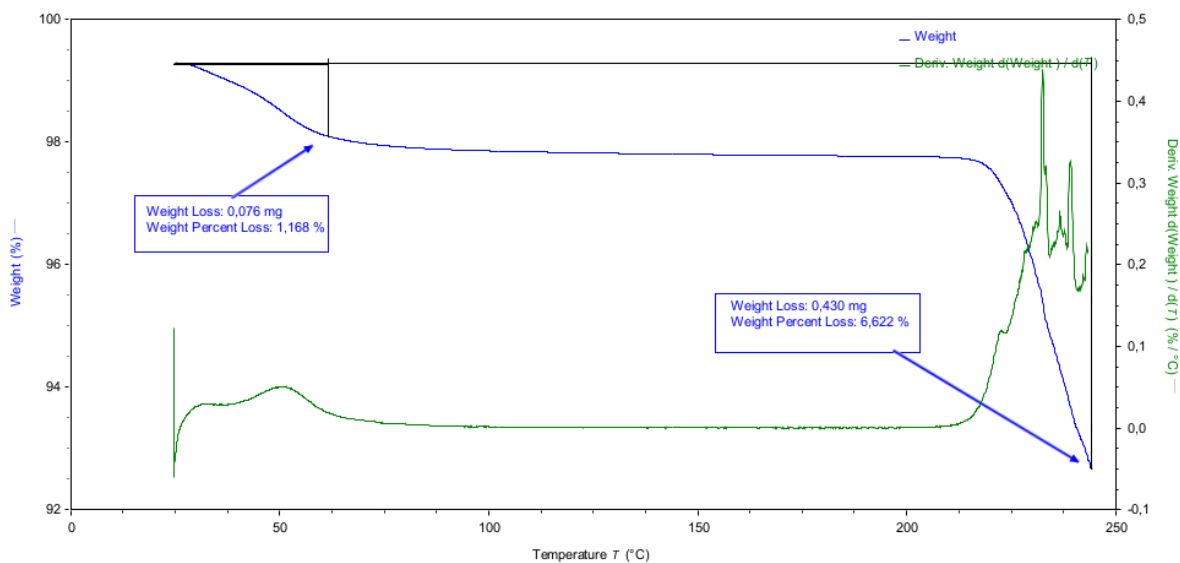


**Figure 3:** TGA spectrum of rifaximin.

Table 4 recapitulates the results of DSC for crystals of rifaximin in seven pure solvents at 10°C/min using closed sample pans, and Figure 4 compares the DSC spectra of crystals obtained for all solid phases, which are similar with respect to the DSC original powder except for ethylene glycol that exhibits an endothermic peak at 114 °C previous to fusion at 194 °C (Figure 4). The TGA graph showed that weight change occurred inversely proportional to temperature rise and occurred continuously.

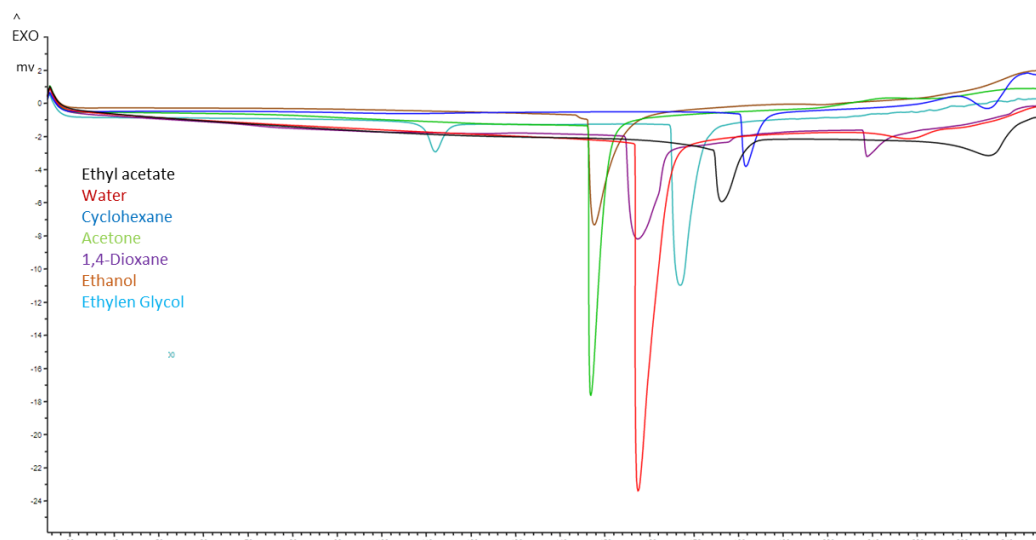


**Figure 4:** DSC spectrum of crystals of rifaximin in pure solvents at 10°C/min using closed sample pans.

**Table 4:** DSC for crystals of rifaximin in pure solvents at 10 °C/min using closed sample pans.

	Rifaximin	Ethyl Acetate	Water	Cyclohexane	Acetone	1,4-Dioxane	Ethanol	Ethylene glycol
<b>Mass (mg)</b>	4.9	4.2	4.0	4.5	4.7	4.2	4.4	4.8
<b>Onset (°C)</b>	198.92	194.46	196.64	190.32	196.20	194.62	196.04	194.60
<b>Peak (°C)</b>	199.46	196.20	197.39	191.64	196.85	197.28	197.66	196.80
<b><math>\Delta H^f</math> (Jg<sup>-1</sup>)</b>	12.25	19.26	134.87	13.28	56.55	53.76	39.51	56.40

At the onset of fusion, there was no heat change, as the weight continued to decrease regardless of the phase change that occurred at fusion (Figure 5). In the TGA for the rest of the solvents studied, the variations in weight loss are between 9 and 6%, values very close to those obtained for the drug.

Additionally, the most appropriate design of the standardized cycle with three hot-cold segments was to detect a new polymorph of rifaximin, in particular a change in value of the melting point in the third segment could indicate the presence of a new and more stable polymorph. Method (a) was used as a starting point. The cooling rate of -40 °C/min failed to produce an endothermic peak, even though an endothermic peak was produced at the beginning of the 3<sup>rd</sup> segment. Hence, the cooling rate was changed to -5 °C for method (b). Method (b) failed to produce a second exothermic peak in the third segment, since the end temperature was too low; hence, this cooling rate was too slow and failed to produce an endothermic peak. Therefore, for method (c) the end temperature was increased to 260 °C.

This allowed the formation of a second exothermic peak. The fact that this occurred at a higher temperature compared to the first exothermic peak could indicate that after the melting of rifaximin in the first segment, upon cooling a new and more stable polymorph of rifaximin was formed. This required more heat energy to melt, hence why the melting temperature was increased. However, the cooling rate was too slow, and no endothermic peak was produced. Therefore, for method (d), the cooling rate was

increased to  $-50\text{ }^{\circ}\text{C}/\text{min}$ .

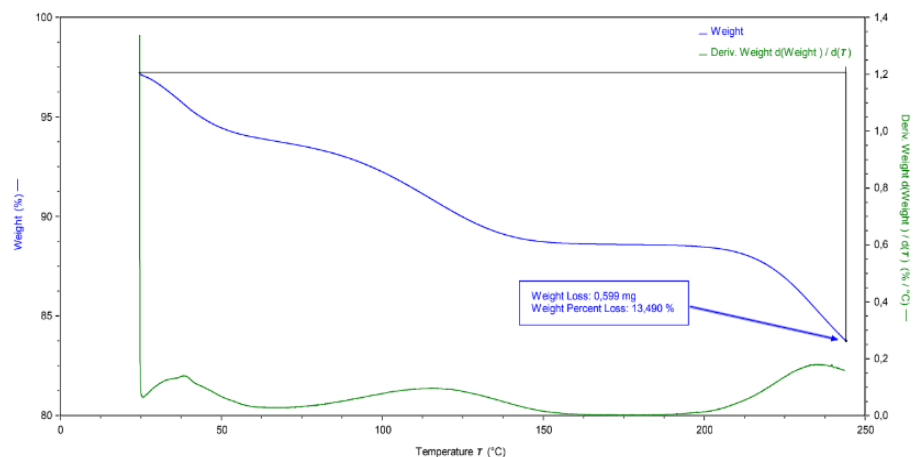


**Figure 5:** TGA of crystals of rifaximin in ethylene glycol.

The increase in the cooling rate led to an increase in the endothermic peak. Though, it was still too broad. Therefore, for method (e), the cooling rate was increased to  $-60\text{ }^{\circ}\text{C}/\text{min}$  with the aim of narrowing the endothermic peak. This cooling rate produced an adequate endothermic peak, therefore it was deemed fit. In attempt to improve this peak, for method (f), a similar method to (e) was used. However, in this case, once the temperature reached  $200\text{ }^{\circ}\text{C}$  in the first segment, this temperature was kept constant for 15 min. This produced a very weak exothermic peak in the first segment and a broader endothermic peak in the second segment.

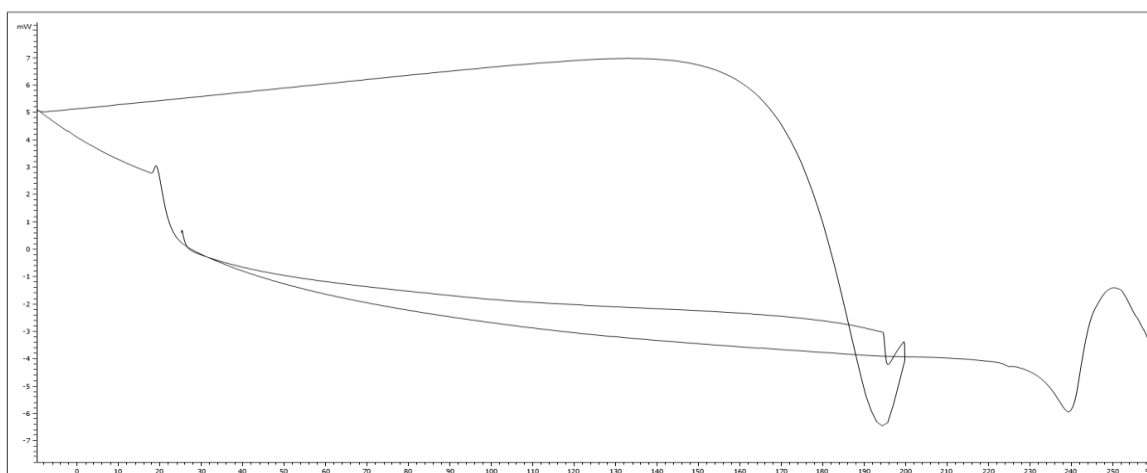


**Figure 6:** DSC spectrum of rifaximin in standardized cycle selected.

Therefore, it was concluded that keeping a constant temperature of  $200\text{ }^{\circ}\text{C}$  for 15 min served no purpose. For method (g), the cooling rate was increased to  $-80\text{ }^{\circ}\text{C}/\text{min}$ , in attempt to further narrow the endothermic peak. This cooling rate produced a narrower endothermic peak when compared to the cooling rate of  $-60\text{ }^{\circ}\text{C}/\text{min}$ . Nevertheless, a small dip was observed in the first segment. To further investigate this, method (h) was used, where the first heating was decreased to  $5\text{ }^{\circ}\text{C}/\text{min}$ . This got rid of the small dip, and it was concluded that this was the optimal heating rate for the first segment (**Figure 6**).



### FT-IR of rifaximin and solid phases

The FT-IR spectra of the pure rifaximin sample and the solid phases in seven pure solvents are shown in Figures 7 and 8. The infrared absorption spectrum of the drug is concordant with the  $\alpha$ -form. In Figure 7, the broad peaks at 3384 and 2938  $\text{cm}^{-1}$  were attributed to the N-H stretching vibration. The broad peak at 3210  $\text{cm}^{-1}$  was attributed to the O-H group that forms part of a carboxylic acid group. The rest of the peaks, which belonged to the fingerprint region, were attributed to C-H, C=C, N-O, O-H, C-O and CO-O-CO groups [24].

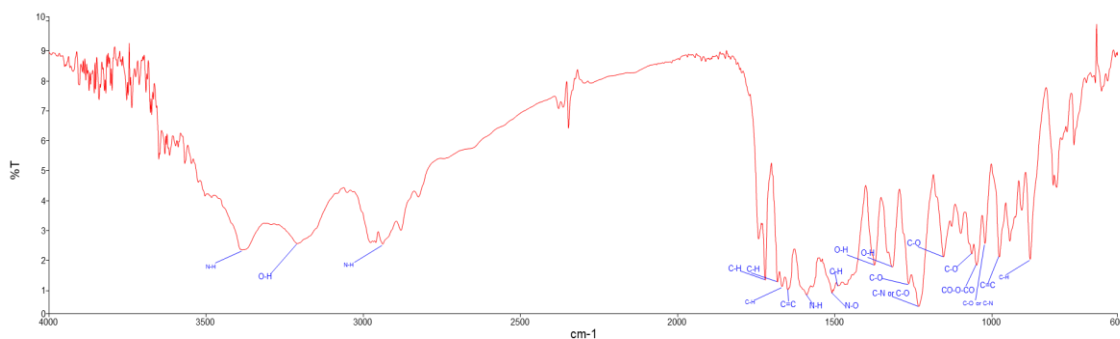


**Figure 7:** FT-IR spectrum of rifaximin.

The results show that none of the selected solvents induces any polymorphic change, which agrees with the results obtained in the DSC, so they could be used in processes to obtain and purify this drug (Figure 8).

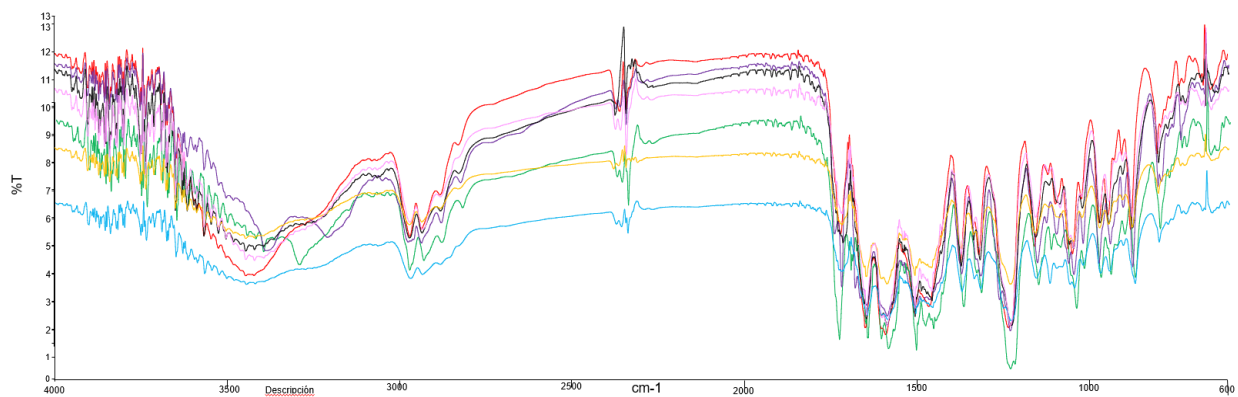


**Figure 8:** FT-IR spectrum of crystals of rifaximin in seven pure solvents (red= water; green= ethyl acetate; purple= cyclohexane; black= acetone; blue = 1,4-Dioxane; orange= ethanol; pink= ethylene glycol).

### Conclusions

Rifaximin represents an excellent example of the close relationship between the solid state and its biopharmaceutical properties. The knowledge of obtaining the polymorphic forms is of the utmost importance and points to the need for greater demands on the part of the regulatory bodies that supervise the identification, obtaining and analysis of the polymorphs of a raw material, which is going to be used in the manufacture of drugs marketed worldwide.

Therefore, a deep understanding of the polymorphic characteristics will allow us to select the best polymorphic form to commercialize. In this work an attempt has been made to obtain new polymorphs of rifaximin from the original raw material, the alpha-form, with the help of different characterization techniques.

## References

1. Cottreau J, Baker SF, DuPoint HL, Garey KW (2010) Rifaximin: a nonsystemic rifamycin antibiotic for gastrointestinal infections. *Expert review of anti-infective. Therapy* 8(7):747-760.
2. Brenner DM, Sayuk GS (2020) Current US food and drug administration-approved pharmacologic therapies for the treatment of irritable bowel syndrome with diarrhea. *Adv Ther* 37(1): 83-96.
3. Bass NM, Mullen KD, Sanyal A, Poordad F, Neff G, et al. (2010) Rifaximin treatment in hepatic encephalopathy. *N Engl J Med* 362(12):1071-1081.
4. Pelosini I, Scarpignato C (2005) Rifaximin, a peculiar rifamycin derivative: established and potential clinical use outside the gastrointestinal tract. *Chemotherapy* 51(1):122-130.
5. Robertson KD, Nagalli S (2022) Rifaximin. Treasure Island, StatPearls Publishing, United States of America.
6. Shayto RH, Mrad RA, Sharara AI (2016) Use of rifaximin in gastrointestinal and liver diseases. *World J Gastroenterol* 22(29): 6638-6651
7. Koo HL, DuPoint HL (2010) Rifaximin: a unique gastrointestinal-selective antibiotic for enteric diseases. *Curr Opin Gastroenterol* 26(1): 17-25.
8. Calanni F, Renzulli C, Barbanti M, Viscomi GC (2014) Rifaximin: beyond the traditional antibiotic activity. *The Journal of Antibiotics* 67:667-670.
9. Viscomi GC, Campana M, Barbanti M, Grepioni F, Polito M, et al. (2008) Crystal forms of rifaximin and their effect on pharmaceutical properties. *Cryst Eng Comm* 10(8):1074-1081.
10. Grant DJW (1999) Theory and origin of polymorphism. In: Brittain HG, editor. *Polymorphism in pharmaceutical solids*. New York, NY, USA: Marcel Dekker.
11. Caira MR (2008) in *Handbook of thermal analysis and calorimetry*. Elsevier.
12. Braga D, Casali L, Grepioni F (2022) The relevance of crystal forms in the pharmaceutical field: sword of damocles or innovation tools? *Int J Mol Sci* 23(16): 9013.
13. Gushurst KS, Yang D, Roe M, Schultheiss N, Vlahova P, et al. (2011) Forms of rifaximin and uses thereof. U.S. Patent No. 8,067,429 B2.
14. Vigano E, Molteni R, Lanfrancioni S, Arrighi M, Gatti, F (2014) Polymorph of rifaximin and process for the preparation there of. U.S. Patent No. 8,877,770 B2.
15. Blandizzi C, Viscomi GC, Scarpignato, C (2014) Impact of crystal polymorphism on the systemic bioavailability of rifaximin, an antibiotic acting locally in the gastrointestinal tract, in healthy volunteers. *Drug Design. Drug Des Devel Ther* 9:1-11.
16. Bianchera A, Nebuloni M, Colombo N, Pirola D, Bettini R (2023) Highly polymorphic materials and dissolution behaviour: the peculiar case of rifaximin. *Pharmaceutics* 15(1): 53.
17. Marzoli G, Federici M, Mascargi M, Maffei P, Calanni F, et al. (2019) Pharmacokinetic differences between alpha rifaximin and a generic rifaximin. *Medicina Interna de México* 35(1): 370-378.

18. Censi R, Di Martino P (2015) Polymorph impact on the bioavailability and stability of poorly soluble drugs. *Molecules* 20(10): 18759-76.
19. Tran TTD, Tran PHL, Park JB, Lee BJ (2012) Effects of solvents and crystallization conditions on the polymorphic behaviors and dissolution rates of valsartan. *Arch Pharm Res* 35: 1223-1230.
20. Tandon R, Tandon N, Gupta N, Gupta R (2018) Art of synthesis of desired polymorphs: A review. *Asian Journal of Chemistry* 30(1): 5-14.
21. Grepioni F, Braga D, Chelazzi L, Shemchuk O, Maffei P. et al, (2019) Improving solubility and storage stability of rifaximin via solid-state solvation with Transcutol®. *Cryst Eng Comm* 21: 5278-5283.
22. Kogawa AC, Salgado HRN (2018) Status of rifaximin: a review of characteristics, uses and analytical methods. *Crit Rev Anal Chem* 48(6): 459-466.
23. Kogawa AC, Antonio SG, Salgado HRN (2016) Characterization of polymorphic forms of rifaximin. *J AOAC Int* 99(4): 964-971.
24. Karanje RV, Bhavsar YV, Jahagirdar KH, Bhise KS (2013) Formulation and development of extended-release micro particulate drug delivery system of solubilized rifaximin. *AAPS Pharm SciTech* 14(2): 639-48.